Cavity enhanced absorption spectroscopy of multiple trace gas species using a supercontinuum radiation source

J. M. Langridge[1], T. Laurila[2], R. S. Watt[2], R. L. Jones[1], C. F. Kaminski[2,3], J. Hult[2,*]

[1]*Department of Chemistry, University of Cambridge, Lensfield Road, Cambridge CB2 1EW, UK*
[2]*Department of Chemical Engineering, University of Cambridge, Pembroke Street, Cambridge CB2 3RA, UK*
[3]*SAOT School of Advanced Optical Technologies, Max-Planck Research Group, University of Erlangen-Nürnberg, D-91058 Erlangen, Germany*
**Corresponding author: jfh36@cam.ac.uk*

Abstract: Supercontinuum radiation sources are attractive for spectroscopic applications owing to their broad wavelength coverage, which enables spectral signatures of multiple species to be detected simultaneously. Here we report the first use of a supercontinuum radiation source for broadband trace gas detection using a cavity enhanced absorption technique. Spectra were recorded at bandwidths of up to 100 nm, encompassing multiple absorption bands of H_2O, O_2 and O_2-O_2. The same instrument was also used to make quantitative measurements of NO_2 and NO_3. For NO_3 a detection limit of 3 parts-per-trillion in 2 s was achieved, which corresponds to an effective 3σ sensitivity of 2.4×10^{-9} $cm^{-1}Hz^{-1/2}$. Our results demonstrate that a conceptually simple and robust instrument is capable of highly sensitive broadband absorption measurements.

OCIS codes: (300.0300) Spectroscopy; (300.1030) Absorption; (120.0120) Instrumentation, measurement, and metrology.

References and links

1. Th. Udem, R. Holzwarth, T. Hänsch, "Optical frequency metrology," Nature **416**, 233-237 (2002).
2. J. Kasparian, M. Rodriguez, G. Méjean, J. Yu, E. Salmon, H. Wille, R. Bourayou, S. Frey, Y.-B. André, A. Mysyrowicz, R. Sauerbrey, J.-P. Wolf, L. Wöste, "White-Light Filaments for Atmospheric Analysis," Science **301**, 61-64 (2003).
3. M. Y. Sfeir, F. Wang, L. Huang, C.-C. Chuang, J. Hone, S. P. O'Brien, T. F. Heinz, L. E. Brus, "Probing Electronic Transitions in Individual Carbon Nanotubes by Rayleigh Scattering," Science **306**, 1540-1543 (2004).
4. A. Unterhuber, B. Považay, K. Bizheva, B. Hermann, H. Sattmann, A. Stingl, T. Le, M. Seefeld, R. Menzel, M. Preusser, H. Budka, C. Schubert, H. Reitsamer, P. K. Ahnelt, J. E. Morgan, A. Cowey, W. Drexler, "Advances in broad bandwidth light sources for ultrahigh resolution optical coherence tomography," Phys. Med. Biol. **49**, 1235-1246 (2004).
5. R. R. Alfano, *The Supercontinuum Laser Source, 2nd ed.* (Springer, New York, 2006).
6. W. H. Reeves, D. V. Skryabin, F. Biancalana, J. C. Knight, P. St. J. Russell, F. G. Omenetto, A. Efimov, A. J. Taylor, "Transformation and control of ultra-short pulses in dispersion-engineered photonic crystal fibres," Nature **424**, 511-515 (2003).
7. P. V. Kelkar, F. Coppinger, A. S. Bhushan, B. Jalali, "Time-domain optical sensing," Electron. Lett. **35**, 1661-1662 (1999).
8. S. T. Sanders, "Wavelength-agile fiber laser using group-velocity dispersion of pulsed super-continua and application to broadband absorption spectroscopy," Appl. Phys. B **75**, 799–802 (2002).
9. J. Hult, R. S. Watt, C. F. Kaminski, "High bandwidth absorption spectroscopy with a dispersed supercontinuum source," Opt. Express **15**, 11385-11395 (2007).
10. M. J. Thorpe, K. D. Moll, R. J. Jones, B. Safdi, J. Ye, "Broadband cavity ringdown spectroscopy for sensitive and rapid molecular detection," Science **311**, 1595-1599 (2006).
11. R. Engeln, G. Berden, R. Peeters, G. Meijer, "Cavity enhanced absorption and cavity enhanced magnetic rotation spectroscopy," Rev. Sci. Instrum. **69**, 3763-3769 (1998).

#95735 - $15.00 USD Received 2 May 2008; revised 10 Jun 2008; accepted 11 Jun 2008; published 23 Jun 2008

12. A. O'Keefe and D. A. G. Deacon, "Cavity ring-down optical spectrometer for absorption-measurements using pulsed laser sources," Rev. Sci. Instrum. **59**, 2544-2551 (1988).
13. J. Ye and J. L. Hall, "Cavity ringdown heterodyne spectroscopy: High sensitivity with microwatt power light power," Phys. Rev A **61**, 061802 (2000).
14. J. Ye and J. L. Hall, "Ultrasensitive detection in atomic and molecular physics: demonstration in molecular overtone spectroscopy," J. Opt. Soc. Am. B **15**, 6-15 (1998).
15. S.M. Ball and R.L. Jones, "Broad-band cavity ring-down spectroscopy," Chem. Rev. **103**, 5239-5262 (2003).
16. J. J. Scherer, J. B. Paul, H. Jiao, A. O'Keefe, "Broadband ringdown spectral photography," Appl. Opt. **40**, 6725-6732 (2001).
17. S. M. Ball, I. M. Povey, E. G. Norton, R. L. Jones, "Broadband cavity ringdown spectroscopy of the NO_3 radical," Chem. Phys. Lett. **342**, 113-120 (2001).
18. M. J. Thorpe, D. D. Hudson, K. D. Moll, J. Lasri, J. Ye, "Cavity-ringdown molecular spectroscopy based on an optical frequency comb at 1.45-1.65 μm," Opt. Lett. **32**, 307-309 (2007).
19. M. J. Thorpe, D. Balslev-Clausen, M. S. Kirchner, J. Ye, "Cavity-enhanced optical frequency comb spectroscopy: application to human breath analysis," Opt. Express **16**, 2387-2397 (2008).
20. T. Gherman and D. Romanini, "Mode–locked cavity–enhanced absorption spectroscopy," Opt. Express **10**, 1033-1042 (2002).
21. T. Gherman, E. Eslami, D. Romanini, S. Kassi, J-C. Vial, N. Sadeghi, "High sensitivity broad-band mode-locked cavity-enhanced absorption spectroscopy: measurement of $Ar^*(^3P_2)$ atom and N_2^+ ion densities", J. Phys. D **37**, 2408-2415 (2004).
22. C. Gohle, B. Stein, A. Schliesser, T. Udem, T. W. Hänsch, "Frequency comb vernier spectroscopy for broadband, high-resolution, high-sensitivity absorption and dispersion spectra," Phys. Rev. Lett. **99**, 263902 (2007).
23. S.E. Fiedler, A. Hese, A. A. Ruth, "Incoherent broad-band cavity-enhanced absorption spectroscopy," Chem. Phys. Lett. **371**, 284-294 (2003).
24. D. S. Venables, T. Gherman, J. Orphal, J. C. Wenger, A. A. Ruth, "High sensitivity in situ monitoring of NO_3 in an atmospheric simulation chamber using incoherent broadband cavity-enhanced absorption spectroscopy," Environ. Sci. Technol. **40**, 6758-6763 (2006).
25. S. M. Ball, J. M. Langridge, R. L. Jones, "Broadband cavity enhanced absorption spectroscopy using light emitting diodes," Chem. Phys. Lett. **398**, 68-74 (2004).
26. G. Meijer, M. G. H. Boogaarts, R. T. Jongma, D. H. Parker, A. M. Wodtke, "Coherent cavity ringdown spectroscopy," Chem. Phys. Lett. **217**, 112-116 (1994).
27. M. Triki, P. Cermak, G. Méjean, D. Romanini, "Cavity-enhanced absorption spectroscopy with a red LED source for NO_x trace analysis," Appl. Phys. B **91**, 195-201 (2008).
28. J. M. Langridge, S. M. Ball, R. L. Jones, "A compact broadband cavity enhanced absorption spectrometer for detection of atmospheric NO_2," Analyst **131**, 916-922 (2006).
29. T. Gherman, D. S. Venables, S. Vaughan, J. Orphal, A. A. Ruth, "Incoherent broadband cavity enhanced absorption spectroscopy in the near-ultaviolet: application to HONO and NO_2," Environ. Sci. Technol. **42**, 890-895 (2008).
30. G. D. Greenblatt, J. J. Orlando, J. B. Burkholder, A. R. Ravishankara, "Absorption measurements of oxygen between 330nm and 1140nm," J. Geophy.Res. **95**, 18577-18582 (1990).
31. A.C. Vandaele, C. Hermans, P. C. Simon, M. Carleer, R. Colin, S. Fally, M. F. Mérienne, A. Jenouvrier, B. Coquart, "Measurements of the NO_2 absorption cross-section from 42000 cm^{-1} to 10000 cm^{-1} (238-1000 nm) at 220 K and 294 K," J. Quant. Spectrosc. Radiat. Transfer. **59**, 171-184 (1998).
32. J. Orphal, C. E. Fellows, P. –M. Flaud, "The visible absorption spectrum of NO_3 measured by high-resolution Fourier transform spectroscopy," J. Geophys. Res. **108**, 4077 (2003).
33. U. Platt, "Modern methods of the measurement of atmospheric trace gases," Phys. Chem. Chem. Phys. **24**, 5409-5415 (1999).
34. E. J. Dunlea, S. C. Herndon, D. D. Nelson, R. M. Volkamer, F. San Martini, P. M. Sheehy, M. S. Zahniser, J. H. Shorter, J. C. Wormhoudt, B. K. Lamb, E. J. Allwine, J. S. Gaffney, N. A. Marley, M. Grutter, C. Marquez, S. Blanco, B. Cardenas, A. Retama, C. R. Ramos Villegas, C. E. Kolb, L. T. Molina, M. J. Molina, "Evaluation of nitrogen dioxide chemiluminescence monitors in a polluted urban environment," Atmos. Chem. Phys. **7**, 2691-2704 (2007).
35. W. R. Simpson, "Continuous wave cavity ring-down spectroscopy applied to in situ detection of dinitrogen pentoxide (N_2O_5)," Rev. Sci. Instrum. **74**, 3442-3452 (2003).
36. J. D. Ayers, R. L. Apodaca, W. R. Simpson, D. S. Baer, "Off-axis cavity ringdown spectroscopy: application to atmospheric nitrate radical detection," Appl. Opt. **44**, 7239-7242 (2005).
37. W. P. Dubé, S. S. Brown, H. D. Osthoff, M. R. Nunley, S. J. Ciciora, M. W. Paris, R. J. McLaughlin, A. R. Ravishankara, "Aircraft instrument for simultaneous, in situ measurement of NO_3 and N_2O_5 via pulsed cavity ring-down spectroscopy," Rev. Sci. Instrum. **77**, 034101 (2006).
38. C. Vallance, "Innovations in cavity ringdown spectroscopy," New J. Chem. **29**, 867-874 (2005).
39. S. A. Diddams, L. Hollberg, V. Mbele, "Molecular fingerprinting with the resolved modes of a femtosecond laser frequency comb," Nature **445**, 627-630 (2007).

#95735 - $15.00 USD Received 2 May 2008; revised 10 Jun 2008; accepted 11 Jun 2008; published 23 Jun 2008

40. E. Sorokin, I. T. Sorokina, J. Mandon, G. Guelachvili, and N. Picque, "Sensitive multiplex spectroscopy in the molecular fingerprint 2.4 μm region with a Cr2+:ZnSe femtosecond laser," Opt. Express **15**, 16540-16545 (2007).
41. A. A. Ruth, J. Orphal, S. E. Fiedler, "Fourier-transform cavity-enhanced absorption spectroscopy using an incoherent broadband light source," Appl. Opt. 46, 3611-3616 (2007)
42. A. Kudlinski, A. K. George, J. C. Knight, J. C. Travers, A. B. Rulkov, S. V. Popov, J. R. Taylor, "Zero-dispersion wavelength decreasing photonic crystal fibers for ultraviolet-extended supercontinuum generation," Opt. Express **14**, 5715-5722 (2006).
43. C. Xia, M. Kumar, O. P. Kulkarni, M. N. Islam, F. L. Terry, M. J. Freeman, M. Poulain, G. Mazé, "Power scalable mid-infrared supercontinuum generation in ZBLAN fluoride fibers with up to 1.3 watts time-averaged power," Opt. Express **15**, 865-871 (2007).
44. S. E. Fiedler, A. Hese, A. A. Ruth, "Incoherent broad-band cavity-enhanced absorption spectroscopy of liquids" Rev. Sci. Instum. **76**, 023107 (2005).
45. M. Mazurenka, L. Wilkins, J. V. Macpherson, P. R. Unwin, S. R. Mackenzie, "Evanescent Wave Cavity Ring-Down Spectroscopy in a Thin-Layer Electrochemical Cell," Anal. Chem. **78**, 6833-6839 (2006).

1. Introduction

Supercontinuum (SC) radiation sources are attractive for spectroscopic applications in physics, chemistry and biology [1-4], owing to their unique combination of high spectral brightness and broadband wavelength coverage [5,6]. These features enable spectral signatures of multiple species to be detected simultaneously. The use of SC radiation in spectroscopic gas sensing applications has so far been restricted to direct absorption techniques [7-9], which can lack the sensitivity required for trace level detection or for the observation of weak spectral features. The detection of trace gases over broad spectral bandwidths is, however, desirable for many applications ranging from atmospheric sensing and industrial process control to medical diagnostics. In order to be as versatile as possible, Thorpe *et al.* proposed that a spectroscopic gas sensing system should fulfill the following criteria [10]: (i) broad spectral bandwidth, ideally 100 nm or more, for target selective multiple species measurements; (ii) high sensitivity for trace level detection; (iii) high acquisition speeds for real-time monitoring applications; and (iv) sufficient spectral resolution for species specificity. To this list of criteria one can also add: (v) a simple and robust design for operation in a diverse range of application environments. Cavity based absorption techniques, which employ high finesse optical cavities to achieve long sample absorption path lengths, have been shown to achieve the high sensitivity required for trace gas detection. A number of experimental schemes including cavity enhanced absorption spectroscopy (CEAS) [11], cavity ringdown spectroscopy (CRDS) [12,13] and noise-immune cavity-enhanced optical heterodyne molecular spectroscopy (NICE-OHMS) [14], have been reported with sensitivities of better than 10^{-10} $cm^{-1}Hz^{-1/2}$. Most implementations of these techniques with coherent light sources have however been restricted to either narrow spectral bandwidths or long acquisition times, thus limiting their capability for fast response multiple species sensing.

Broadband CRDS, in which an optical cavity containing the absorption sample is excited by a short broadband radiation pulse, with the subsequent decay of light exiting the cavity monitored simultaneously in both time and wavelength, has been demonstrated by a number of groups [15]. Experiments have used broadband pulsed dye lasers together with schemes for simultaneous time and wavelength resolved detection based on either a rapidly scanned mirror, diffraction grating and charge coupled device (CCD) camera [16], or a grating spectrometer and time resolved CCD camera employing controlled on-chip charge transfer [17]. Acquisition of single-shot spectra covering 15 nm have been demonstrated using such schemes [16].

Even broader bandwidths have recently been achieved, both in the visible and near-infrared (IR) spectral regions, using optical frequency comb radiation sources [10,18,19]. Multiple species trace level detection over spectral bandwidths of around 100 nm has been achieved using a frequency comb CRDS instrument [10,18]. The broad wavelength coverage was achieved by employing a scanning grating spectrometer and a single element detector, which resulted in long acquisition times. However, the frequency comb CRDS scheme has

#95735 - $15.00 USD Received 2 May 2008; revised 10 Jun 2008; accepted 11 Jun 2008; published 23 Jun 2008

also been combined with a rapidly scanned mirror/CCD camera detection approach to achieve much faster acquisition times (~1ms), albeit over a more modest spectral bandwidth (15 nm) [10].

Furthermore, optical frequency combs have been employed for CEAS measurements, where the steady state intensity transmitted by an optical cavity under continuous wave excitation is monitored. In the visible spectral region a bandwidth of 4 nm has been achieved using a grating spectrometer for detection [20], with similar performance demonstrated in the near-UV spectral region [21]. In the near-IR, multiple species detection over 200 nm (divided into sequentially recorded 25 nm sections) at a spectral resolution of 0.8 GHz has also been demonstrated using a virtually imaged phased array spectrometer [19].

It is prudent to note that when employing an optical frequency comb for cavity absorption measurements, the frequency comb must be actively matched with the mode structure of the high finesse cavity to ensure that the comb components are resonantly coupled into the cavity modes. While this requirement enables extremely efficient coupling of radiation into the cavity, it also introduces significant experimental complexity, which somewhat compromises the robustness of instruments for field applications. An interesting alternative approach is to use a frequency comb in combination with a scanning enhancement cavity to achieve high resolution multi-wavelength measurements. A Vernier spectrometer based on this principle was recently demonstrated covering a bandwidth of 8 nm at a spectral resolution of 1 GHz [22].

Broadband CEAS has also been demonstrated using incoherent light sources, such as light emitting diodes (LED) and Xe arc lamps [23]. High sensitivity CEAS measurements covering spectral ranges of 100 nm using a lamp [24], and 60 nm using an LED [25] have been reported. These approaches facilitate the production of compact, robust and low cost instrumentation, however, the low spectral brightness of incoherent sources ultimately forces the use of either increased integration times, or cavity lengths, to achieve sensitivities comparable to those that can be attained using a supercontinuum source.

In this article, we report upon a broadband CEAS scheme using a supercontinuum source that is capable of acquiring spectra over bandwidths of 100 nm in seconds. The sensitivity of the instrument is demonstrated through trace level detection of NO_2 and NO_3, with a 3σ detection limit of 3 parts per trillion by volume (pptv) achieved for NO_3. The technique is conceptually simple and fulfils all the criteria for multi-species trace gas sensing outlined above. The use of a SC light source gives access to a very wide spectral window, here covering more than 1500 nm in the visible and near-IR spectral regions. In addition, the use of a non-confocal cavity alignment yields a quasi-continuous mode structure [26], which combined with the dense mode structure of the supercontinuum source (here 10 MHz), ensures broadband cavity transmission without the requirement for any active longitudinal cavity mode matching. This represents a significant simplification with respect to the mode matched approaches discussed above and allows for a robust experimental set-up. The disadvantage of this scheme is the reduced efficiency with which light is coupled into the optical cavity [27]. However, this is compensated by the high spectral brightness of modern SC sources, and in the work presented here, sufficient photon fluxes for high sensitivity broadband CEAS measurements were obtained in signal integration times of 2 s. Finally, it is noted that the CEAS scheme does not require extremely fast temporal resolution in the detection system, so enabling the use of conventional array detectors.

2. Spectrometer set-up and operation

The experimental set-up for supercontinuum based cavity enhanced absorption spectroscopy is shown in Fig. 1. The light source is a SC fibre laser (Fianium SC400) with a 10 MHz repetition rate, which determines the SC mode spacing, and 2 Watt nominal average output power. An achromatic lens is employed to collimate the SC radiation, which exits the photonic crystal fibre (PCF) used for its generation, into a beam with a diameter of 2.5 mm and a M^2 factor of about 1.1. The divergence of the collimated beam is wavelength dependent,

#95735 - $15.00 USD Received 2 May 2008; revised 10 Jun 2008; accepted 11 Jun 2008; published 23 Jun 2008

and the collimation is therefore optimised for operation at visible wavelengths. The SC spectrum extends from 400 nm to above 2000 nm, which provides access to a very wide spectral region. In this work, however, limitations imposed by the high reflectivity bandwidth of available cavity ringdown mirrors imposed an upper limit to the working wavelength range of approximately 100 nm. Nevertheless, within these bounds the performance of the supercontinuum based CEAS approach is explored, and extension to wider bandwidths is discussed in section 4. The SC radiation is spectrally filtered to match the bandwidth of the high reflectivity cavity mirrors. First the visible part of the output is isolated using a combination of an IR separation unit (Fianium) and a hot mirror (Comar 716 GK 25). Then a spectral bandwidth of about 100 nm is isolated using an interference filter centred at 670 nm (Comar 670 IW 12), see Fig. 2 (a). The total power available after filtering is around 7 mW. The duration of the ytterbium based fibre laser master pump source is about 5 ps, whereas the 100 nm wide spectrally filtered SC pulses are estimated to be broadened to around 200 ps due to dispersion in the PCF.

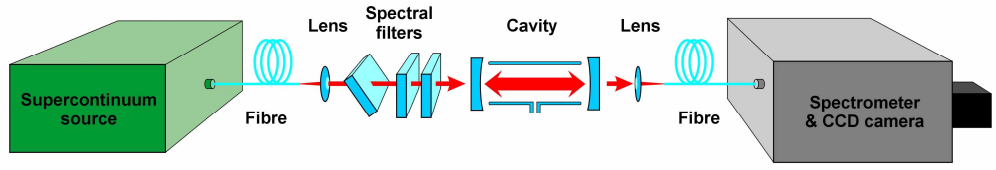

Fig. 1. Experimental set-up for broadband SC-CEAS. For spectral filtering a combination of a beamsplitter, a hot mirror and a broadband interference filter was employed. Beam steering mirrors used to direct the filtered SC radiation into the cavity are not shown.

The light is passively coupled into a 1.15 m long optical cavity formed by two highly reflective mirrors (Los Gatos Research, 99.995 % nominal reflectivity at 660 nm, 1 m radius of curvature). No effort is made to spatially match the supercontinuum beam to the fundamental TEM_{00} mode of the cavity, and therefore higher-order transverse modes are also excited. This is desirable for broadband experiments, as for a cavity length away from the confocal arrangement the transverse and longitudinal mode spacing is non-degenerate, and thus yields a dense quasi-continuous mode structure resulting in a finite transmission at all wavelengths [26].

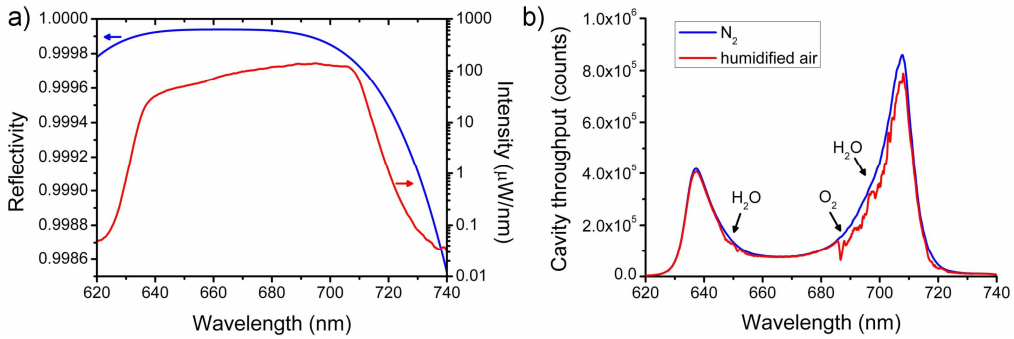

Fig. 2. (a) Measured mirror reflectivity curve (blue) and filtered SC output (red), (b) cavity throughput corresponding to the empty cavity (N_2 flushed) and filled cavity (humidified air).

A 1 inch diameter, 1.14 m long glass tube is positioned between the cavity mirrors to enable the cavity volume to be purged with controlled synthetic gas mixtures during experiments. All experiments reported here were performed at atmospheric pressure. The light transmitted through the cavity, see Fig. 2 (b), is collected by a plano-convex achromatic lens (Newport PAC040), coupled into a multimode fibre (d=400 μm) and spectrally dispersed

#95735 - $15.00 USD Received 2 May 2008; revised 10 Jun 2008; accepted 11 Jun 2008; published 23 Jun 2008

using a grating spectrometer (PI Acton SP2300). For broad spectrometer coverage (130 nm) a 600 grooves/mm grating is employed, which results in a resolution of 0.3 nm full width half at maximum (FWHM). For higher resolution experiments, a 1800 grooves/mm grating is used, which provides a spectral coverage of 28 nm at 0.1 nm FWHM resolution. Wavelength calibration of the spectrograph is performed using Ne atomic emission lines, which are also used to define the instrument's slit function. An air cooled CCD camera (PI Acton Pixis 400B, 1340×400 pixels) is used to record spectra with an on chip integration time of 2 seconds, corresponding to the average of 20 million supercontinuum pulses. Each spectral element of the CCD detector records data averaged over thousands of laser and cavity modes, which further acts to wash out any effects of resonant mode coupling.

The short term stability of the instrument was assessed by evaluating the cavity throughput intensity over 100 consecutive 2 s spectra acquired as the cavity was flushed with dry N_2. The standard deviation of the throughout intensity was calculated for each CCD pixel within the range 630 – 720 nm. The stability was found to vary between 0.2 and 0.5 % across the wavelength range, which reflected the change in absolute light intensity reaching the detector. The stability over longer acquisition periods, which will ultimately determine the frequency with which calibration of the instrument is necessary, will form the subject of a future study.

CEAS experiments were performed by measuring the steady state intensity transmitted by the optical cavity both in the presence (I) and absence (I_0) of an absorbing sample. The latter condition was met by purging the cavity volume with dry nitrogen. The sample absorption coefficient $\alpha(\lambda)$ was subsequently determined from [23]

$$\alpha(\lambda) = \left(\frac{I_0(\lambda)}{I(\lambda)} - 1 \right) \frac{1 - R(\lambda)}{d} \tag{1}$$

where d is the cavity mirror to mirror separation distance and $R(\lambda)$ the wavelength dependent cavity mirror reflectivity.

As indicated by Eq. (1), in order to calculate absolute absorber concentrations from CEAS intensity measurements, the reflectivity of the cavity mirrors must be determined. In previous broadband CEAS experiments, methods adopted for this purpose have included the direct measurement of $R(\lambda)$ by broadband cavity ringdown spectroscopy using pulsed radiation from a broadband dye laser together with time resolved CCD detection [25]. An alternative approach used CEAS measurements of absorption by a species present within the cavity at a well defined concentration, e.g. O_2-O_2 [28] or NO_2 [29]. With knowledge of the species' absorption cross section, the sample absorption coefficient could be calculated, which subsequently enabled $R(\lambda)$ to be determined indirectly from inversion of Eq. (1). The later method is advantageous, firstly as it requires no additional experimental equipment beyond that already used for CEAS measurements, but more fundamentally because $R(\lambda)$ is determined using the same light source and cavity excitation geometry used for sample CEAS measurements. This is of importance because the effective magnitude of $R(\lambda)$ depends upon the range of transverse cavity modes excited by the input radiation. In the current work, a variant of the later method using absorption by both O_2-O_2 and NO_2 was adopted. This method has been applied previously to broadband LED based CEAS experiments [28] and is described only briefly here.

Firstly, the known collision-induced absorption by the O_2-O_2 dimer [30] was measured in pure oxygen around 630 nm, which allowed the absolute value of the mirror reflectivity to be determined at this wavelength. The *relative* mirror reflectivity profile across the remainder of the measurement bandwidth (620-740 nm) was subsequently determined from the structure of the wide bandwidth spectrum of NO_2 [31] present at an arbitrary concentration. The absolute mirror reflectivity was then obtained by constraining the relative reflectivity to the absolute measurement at 630 nm. In principle, the mirror reflectivity could have been determined directly from NO_2 present at a known concentration, however NO_2 is readily lost to surfaces

#95735 - $15.00 USD Received 2 May 2008; revised 10 Jun 2008; accepted 11 Jun 2008; published 23 Jun 2008

making the preparation of such a sample technically challenging. Figure 2 (a) shows the determined mirror reflectivity, which peaks at R=0.99994 around 660 nm, corresponding to an effective cavity ringdown time of 64 μs and an effective absorption path within the 1.15 m long optical cavity of 19.2 km. The uncertainty in the derived mirror reflectivity propagates to subsequent CEAS measurements through the (1-$R(\lambda)$) factor detailed in Eq. 1. The estimated total uncertainty in (1-$R(\lambda)$) is 8%, with contributions arising from the uncertainty in the O_2 pressure within the cavity (5%), the O_2-O_2 absorption cross section (2%), the cavity length (1%) and the errors associated with the I_0/I term in Eq. 1 (0.5%) and the retrieval of O_2 concentrations from measured spectra (2%).

3. Proof of principle measurements

3.1 Qualitative spectra illustrating the wavelength coverage of the SC-CEAS instrument

Initial experiments sought to demonstrate the broad spectral coverage of SC-CEAS by probing multiple absorption features of H_2O and O_2. Humidified air was generated by bubbling synthetic air (Air Liquide) through a water bubbler at a rate of 5 litres per minute. Independent humidity measurements performed using a commercial thermohygrometer (Vaisala HMP41) indicated a sample relative humidity of 77% at 23°C. Figure 3 shows an example spectrum, which simultaneously captures two vibrational overtone bands of H_2O and three electronic transitions of O_2 and O_2-O_2, detected across a 100 nm acquisition range. The bandwidth, limited here by the working wavelength ranges of the cavity mirrors and spectrometer, compares favorably with alternative broadband CEAS setups and exceeds that of any other coherent source arrangements. The extension to even wider wavelength coverage, where the potential of the SC source could be more fully exploited, is discussed in section 4.

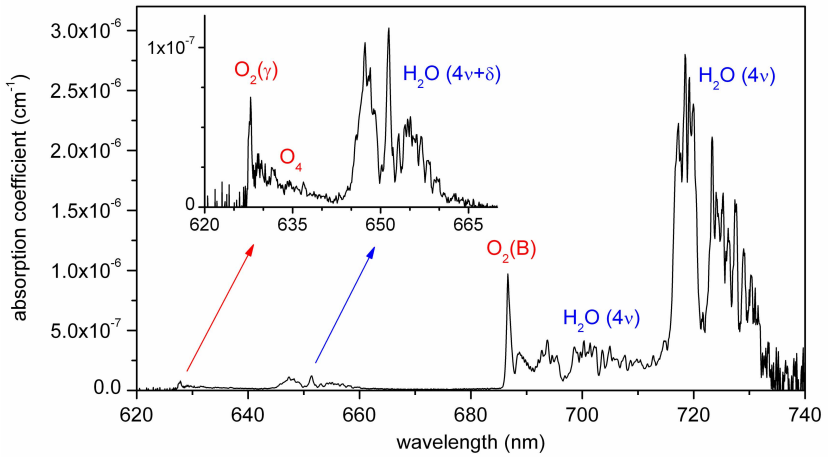

Fig. 3. Broadband SC-CEAS spectrum of synthetic air humidified to 77% RH at 23°C. The spectrum captures 100 nm of spectral information at a resolution of 0.3 nm FWHM and was acquired in a single measurement with an integration time of 2 s. The baseline region of the spectrum where no absorption features are found (663-683 nm) has a standard deviation of 1.6×10^{-9} cm^{-1}.

Figure 4 shows higher resolution spectra of both the H_2O 4ν and 4ν+δ polyads, measured in synthetic air humidified to 40% relative humidity at 23°C, and the O_2 B band, recorded in dry synthetic air. In principle, the absorber concentration could be determined from each spectrum by fitting the measured absorption structure to reference H_2O/O_2 absorption cross sections. However, this procedure is complicated here as both the H_2O and O_2 absorption linewidths are significantly narrower than the sampling resolution of the CEAS instrument (typically 0.005 nm and 0.01 nm FWHM for H_2O and O_2 respectively compared to the instrument resolution of 0.1 nm FWHM). Consequently, the instrument is unable to resolve

#95735 - $15.00 USD Received 2 May 2008; revised 10 Jun 2008; accepted 11 Jun 2008; published 23 Jun 2008

the saturation of strong H_2O and O_2 lines which occurs over the long absorption path lengths encountered within the cavity. The net result is the distortion of measured absorption structure away from that expected from the convolution of the high resolution H_2O/O_2 absorption cross sections with the instrument slit function. Similar complications affecting broadband CRDS spectra of H_2O and O_2 have been discussed in detail previously, together with a method for the analysis of affected spectra [15]. However, the adaptation of this method to the analysis of broadband CEAS spectra lies beyond the purpose of this work.

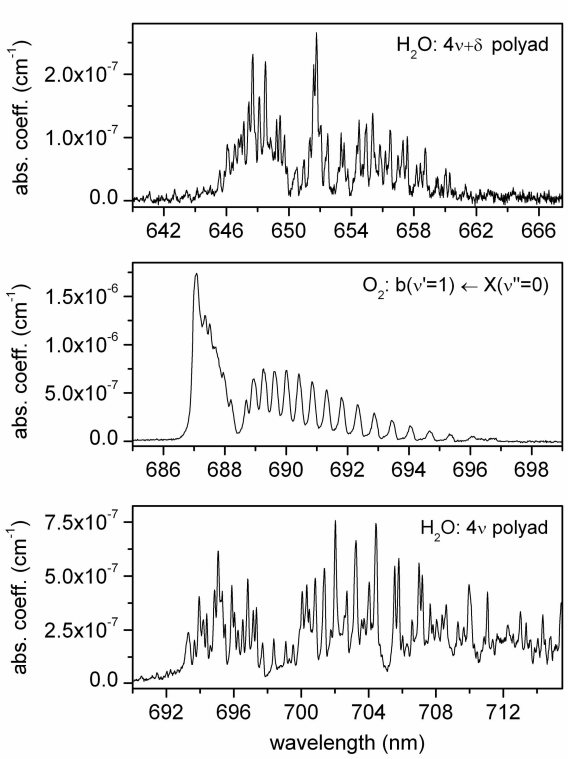

Fig. 4. High resolution SC-CEAS spectra of the 4ν and 4ν+δ polyad vibrational overtones of water vapour and the oxygen B band. The spectra were acquired in an integration time of 2 s at a resolution of 0.1 nm FWHM. The baseline of the O_2 spectrum (685-686.5 nm) has a standard deviation of 4.7×10^{-9} cm^{-1}.

3.2 Quantitative trace level detection of NO_2 and NO_3 using SC-CEAS

Further experiments were performed to demonstrate the sensitivity of SC-CEAS through trace level measurements of two molecules of particular importance in the atmospheric sciences, NO_2 and NO_3. Measurements were performed in the wavelength region 640-675 nm, where both molecules exhibit well structured absorption [31,32]. NO_2 samples were prepared by diluting a small flow of NO_2 from a cylinder source (BOC, 50 ppm) into a 5 litres per minute carrier flow of dry nitrogen. NO_3 samples were prepared from the thermal decomposition of N_2O_5 entrained into a flow of dry nitrogen as it passed over crystalline N_2O_5 held within a dry ice cold trap.

Absorber concentrations were retrieved from measured broadband spectra by differential fitting, as routinely applied to differential optical absorption spectroscopy [33]. Firstly, the NO_2 absorption cross section was reduced to the resolution of the CEAS instrument by convolution with the measured instrument slit function. This procedure was not necessary for the broad NO_3 absorption feature which contains no high resolution structure. The NO_2/NO_3 absorption cross sections were used to analyse data by fitting the following equation to the

#95735 - $15.00 USD Received 2 May 2008; revised 10 Jun 2008; accepted 11 Jun 2008; published 23 Jun 2008

measured absorption structure using a Levenberg-Marquardt routine, $\alpha(\lambda) = n_x\sigma_x(\lambda) + a\lambda^2 + b\lambda + c$, where x is NO_2 or NO_3, n the molecular number density (molecule cm^{-3}) and σ the absorption cross section (cm^2). The absorber's number density was subsequently converted to a volume mixing ratio by dividing n_x by the total molecular density at 1 atmosphere pressure. The addition of polynomial fitting coefficients *a*, *b* and *c* accounted for smoothly varying background contributions to the measured spectra.

Figure 5 (a) shows a spectrum of NO_2, together with a fit to the measured absorption structure that retrieves a NO_2 concentration of 125 parts per billion by volume (ppbv). This spectrum illustrates that the performance of the current instrument is already sufficient for environmental monitoring applications in urban environments, where NO_2 concentrations of several 10s ppbv are common [34]. Despite this, it is noted that the 640-675 nm operating spectral region provides far from optimal sensitivity for NO_2 detection. Around 500 nm the differential absorption cross section of NO_2 is some 10-15 times larger [31] and would yield a corresponding 10-15 times improvement in sensitivity. The precision with which the absorber concentration was retrieved is 0.7 ppbv (0.6%), which indicates the statistical error associated with the spectral fitting procedure. The total uncertainty is somewhat larger than this and is dominated by systematic contributions from the mirror reflectivity calibration (8% uncertainty in 1-$R(\lambda)$ term) and the NO_2 absorption cross section (3%). Also shown in Fig. 5 (a) is the residual spectrum, calculated from the difference between the measured and fitted spectra. It has a standard deviation 3.5×10^{-9} cm^{-1}, which further indicates the low baseline noise level of the measurements.

Figure 5 (b) shows a spectrum of 38 pptv NO_3. It demonstrates trace level NO_3 detection at a sensitivity sufficient for ambient sensing in the nocturnal planetary boundary layer. The precision of the fit is 0.8 pptv (2.1%), which is again smaller compared to uncertainties associated with the mirror reflectivity calibration (8%) and the NO_3 absorption cross section (10%).

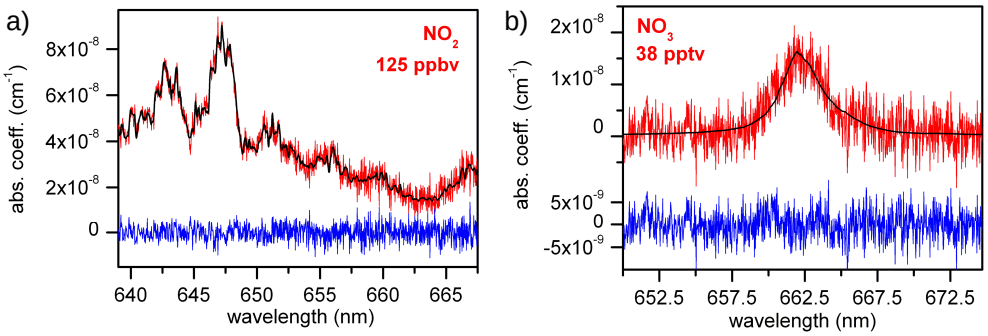

Fig. 5. SC-CEAS spectra of a) NO_2 and b) NO_3. Each spectrum (red) was fitted (black) to retrieve the respective absorber concentrations shown. The residuals (blue) have standard deviations of 3.5×10^{-9} cm^{-1} and 3.2×10^{-9} cm^{-1} for NO_2 and NO_3 respectively. Spectra were acquired at a resolution of 0.1 nm FWHM in a 2 s integration time.

3.3 Evaluation of the instrument's detection limit for NO_3

A quantitative assessment of the instrument's detection sensitivity was conducted using NO_3 as an example target molecule. The sensitivity was estimated by retrieving NO_3 absorber concentrations from consecutive spectra acquired as the cavity was purged with dry N_2. Here, as both I_0 and I were recorded under identical conditions, the resulting spectra contained no NO_3 absorption structure and were composed solely of characteristic instrument noise. Nevertheless, a NO_3 concentration was retrieved from each spectrum (as described in section 3.2) and the detection sensitivity estimated from the statistical spread of concentration values about the 0 pptv level.

#95735 - $15.00 USD Received 2 May 2008; revised 10 Jun 2008; accepted 11 Jun 2008; published 23 Jun 2008

Figure 6 shows the time series of NO_3 concentrations retrieved from 95 consecutive spectra, acquired in a total acquisition period of 190 s. Also shown is a histogram of the concentration distribution, which is characterised by a Gaussian distribution with a 1σ width of 1.0 pptv.

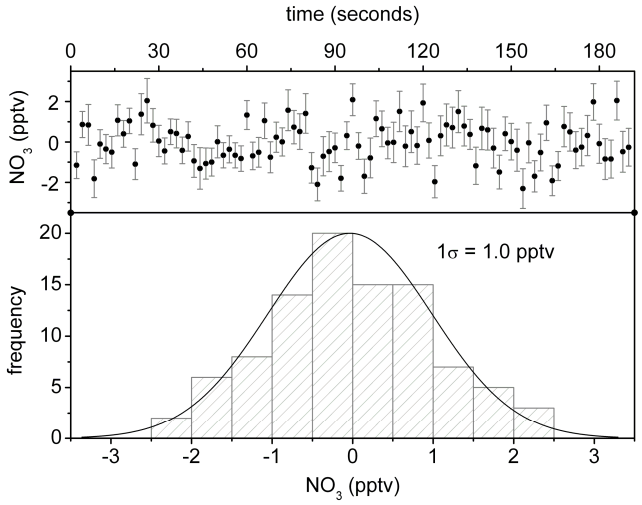

Fig. 6. Time series of NO_3 concentrations retrieved from consecutive 2 s spectra characteristic of the instrument's baseline noise level (upper panel). The standard deviation of the NO_3 concentration distribution (lower panel) indicates a 3σ detection limit of 3 pptv.

Estimating the NO_3 detection sensitivity as three times the standard deviation indicates a limit of 3 pptv in a 2 s acquisition time. This measurement lends itself to compare the performance of the broadband SC-CEAS approach to that of equivalent single wavelength measurements of NO_3 made by conventional cavity ringdown spectroscopy. Noting that the peak NO_3 cross section at 662 nm is 2.2×10^{-17} $cm^2molecule^{-1}$ [32], one finds that a 3 pptv detection limit corresponds to an effective single wavelength minimum detectable absorption coefficient of 2.4×10^{-9} $cm^{-1}Hz^{-1/2}$. This value is lower than that obtained from (3 times) the standard deviation of the residual spectrum shown in Fig. 5 (1.4×10^{-8} $cm^{-1}Hz^{-1/2}$), which indicates the effective gain in sensitivity that arises from adopting a spectrally broadband approach. It also shows that the performance of the broadband SC-CEAS method is comparable to the generally more complex and less flexible single wavelength cavity based techniques, for which absorption sensitivities (1σ) in the range 7×10^{-10} - 4×10^{-11} $cm^{-1}Hz^{-1/2}$ have been reported for NO_3 [35-37].

4. Conclusions

An experimental scheme using a supercontinuum source for highly sensitive broadband cavity enhanced absorption spectroscopy was demonstrated for the first time. Trace level measurements of a range of gas phase species were performed at spectral bandwidths of up to 100 nm. In addition, a quantitative 3σ detection limit for NO_3 of 3 pptv in 2 s was determined, corresponding to a minimum detectable absorption coefficient of 2.4×10^{-9} $cm^{-1}Hz^{-1/2}$ for an equivalent single wavelength measurement of NO_3 performed at 662 nm. The performance of the technique, together with its conceptual simplicity and robust nature, make it ideally suited to a range of gas phase sensing applications. In addition, a number of improvements are possible which would push the technique towards even higher detection sensitivity and wider spectral coverage. For example, optical throughput, and thus sensitivity, could be improved by employing SC sources of higher spectral brightness and by more energy efficient spectral filtering. In order to extend the spectral bandwidth of measurements, the limit imposed by the

#95735 - $15.00 USD Received 2 May 2008; revised 10 Jun 2008; accepted 11 Jun 2008; published 23 Jun 2008

high reflectivity range of conventional cavity ringdown mirrors (ca 100 nm) must be overcome. Potential options include the simultaneous excitation of multiple cavities, each optimised for different wavelength regions, or the use of optical cavities based on total internal reflection [38]. Such developments would enable the full potential of the supercontinuum source for broadband spectroscopy to be exploited. The spectral resolution of measurements could also be improved, while maintaining broadband spectral coverage, by using an echelle spectrometer, a virtually imaged phased array spectrometer [19,39], or a Fourier transform spectrometer [40, 41] in place of the standard grating spectrometer employed here.

Despite the initial demonstration of the technique being performed at visible wavelengths, the SC-CEAS method is by no means limited to the visible part of the spectrum, as SC generation has been demonstrated extending from the UV [42] to the mid-IR [43] spectral region. Extension into the latter is of particular interest for trace gas sensing as many gaseous species of interest exhibit strong transitions at mid-IR wavelengths. An additional exciting avenue for development lies with application of the technique to liquid phase absorption measurements [44], or surface adsorption phenomena studied using an approach akin to evanescent wave cavity ringdown spectroscopy [45]. The broad bandwidth, high sensitivity and fast time resolution of SC-CEAS make it potentially very well suited to applications in each of these fields.

Acknowledgments

This work was funded by the EPSRC (EP/C012488/1) and NERC (NE/C511599/1). The research leading to these results has also received funding from the European Community's Seventh Framework Programme ([FP7/2007-2013] under grant agreement no [PIEF-GA-2008-221538]). JML acknowledges the NERC for support through a PhD studentship. TL acknowledges the support from the Alfred Kordelin Foundation and the Academy of Finland. CFK is thankful to the EPSRC for the provision of a PLATFORM grant and to the Leverhulme trust for personal sponsorship. JH was supported by an Advanced Research Fellowship (EP/C012399/1) from the EPSRC.

#95735 - $15.00 USD Received 2 May 2008; revised 10 Jun 2008; accepted 11 Jun 2008; published 23 Jun 2008